HRTEM and HRSTEM Investigations of oxide thermoelectric materials

Miran Čeh (1), Sašo Šturm (2), Boštjan Jančar (3), Aleksander Rečnik (2), Nina Daneu (2), Goran Dražić (4), Marja Jerič (2), Mateja Košir (2), Matej Presečnik (2), Slavko Bernik (2), Cleva Ow-Yang (5), Mehmet A. Gülgün (5), Johannes de Boor (6)

1) Nanostructured Materials, Jožef Stefan Institute, Ljubljana, Slovenia, Center for Electron Microscopy, Jožef Stefan Institute, Jamova cesta 39, 1000 Ljubljana, Slovenia
2) Nanostructured Materials, Jožef Stefan Institute, Jamova cesta 39, 1000 Ljubljana, Slovenia
3) Advanced Materials, Jožef Stefan Institute, Jamova cesta 39, 1000 Ljubljana, Slovenia
4) National Institute of Chemistry, Hajdrihova ulica 19, 1000 Ljubljana, Slovenia
5) Sabanci University, Orta Mahalle, Üniversite Caddesi No:27 Tuzla, 34956 İstanbul, Turkey
6) German Aerospace Center, Cologne, Germany

Keywords: thermoelectrics, planar faults, modulated structures, HR (S)TEM

It is known that thermoelectric (TE) properties (i.e. figure of merit, ZT) of oxide-based TE materials can be improved by introducing planar faults and/or modulated structures into the matrix material which reduce thermal conductivity via enhanced phonon scattering. In order to tailor TE properties of materials, it is prerequisite to assess structural and chemical information of such nanostructures on atomic scale. In our work we used high-resolution electron microscopy techniques (HRTEM, HRSTEM) accompanied with spectroscopic techniques (EELS and EDS) to characterize the following planar faults and modulated structures in oxide based thermoelectric materials: Ruddlesden-Popper (RP) type planar faults (1) in CaO-doped $Sr(Ti,Nb)O_{3-\delta}$ (STNO), inversion boundaries (IB's) (2) in $ZnO_k(In_2O_3/Al_2O_3)$ and modulated structures in $Ca_3Co_4O_9$-Na_xCoO_{2+x} system (3). All results were obtained in a Jeol 2010F and in Jeol ARM-200CF with Cs probe corrector. TEM BF imaging of CaO-doped STNO showed regions with ordered RP faults and regions with a network of random RP planar faults. HAADF analysis of the perovskite matrix additionally showed that the Nb content on the Ti sites largely varied from app. X=0.05 to X=0.35 for the STNO compositions with 10 mol% of added CaO. Furthermore, the concentration of Ca at the RP faults was always higher as compared to the STNO matrix (Fig. 1). This was attributed to preferential incorporation of smaller Ca ions into the rock-salt-type structure of the RP faults. Within In_2O_3-doped ZnO grains pure In monolayers

parallel to the {0001} ZnO lattice planes were readily observed by the HAADF. These basal inversion boundaries (b-IB) separate domains with different orientation. On the other hand, the pyramidal IB's (p-IB) were much easier observed with ADF due to additional strain contrast caused by In incorporation in these IB's. When some fraction of In_2O_3 was replaced by Al_2O_3, the EDS spatial difference showed that Al is incorporated into the b-IB's as well as into p-IB's (Fig. 2a,b,c,d). The ADF of the $Ca_3Co_4O_9$-Na_xCoO_{2+x} layered cobaltate system revealed coherent intergrowth of two structural types within individual grains. The intergrowths are comprised of the Na_xCoO_2-type where the CoO_2 layers are separated by a layer of Na^+ ions and the $Ca_3Co_4O_9$-type in which the CoO_2 layers are separated by three-layer rock-salt-type structure consisting of one CoO and two CaO layers. The two structural types are intergrown through the octahedral CoO_2 layer (Fig. 2e,f,g). STEM further revealed that Ca incorporates between the CoO_2 layers of Na_xCoO_2 structural part of the grain, thus increasing complexity of interlayer space. Employing EELS we found that differences in local interlayer structure do not affect the oxidation state of Co within the CoO_2 octahedral layers. Finally, TE measurements of above investigated materials confirmed that the presence of planar faults and/or modulated structures increased the ZT value.

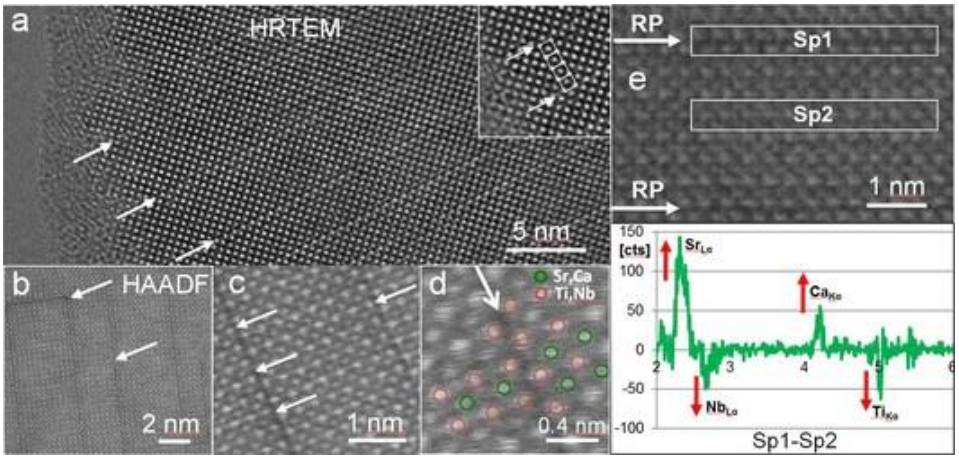

Figure 1. (a) HRTEM of RP faults in CaO-doped STNO. The inset marks four perovskite unit cells in between two RP faults. (b,c,d) HAADF STEM images RP faults that run along {001} perovskite planes. (e) Region of EDS analysis and spatial difference spectrum.

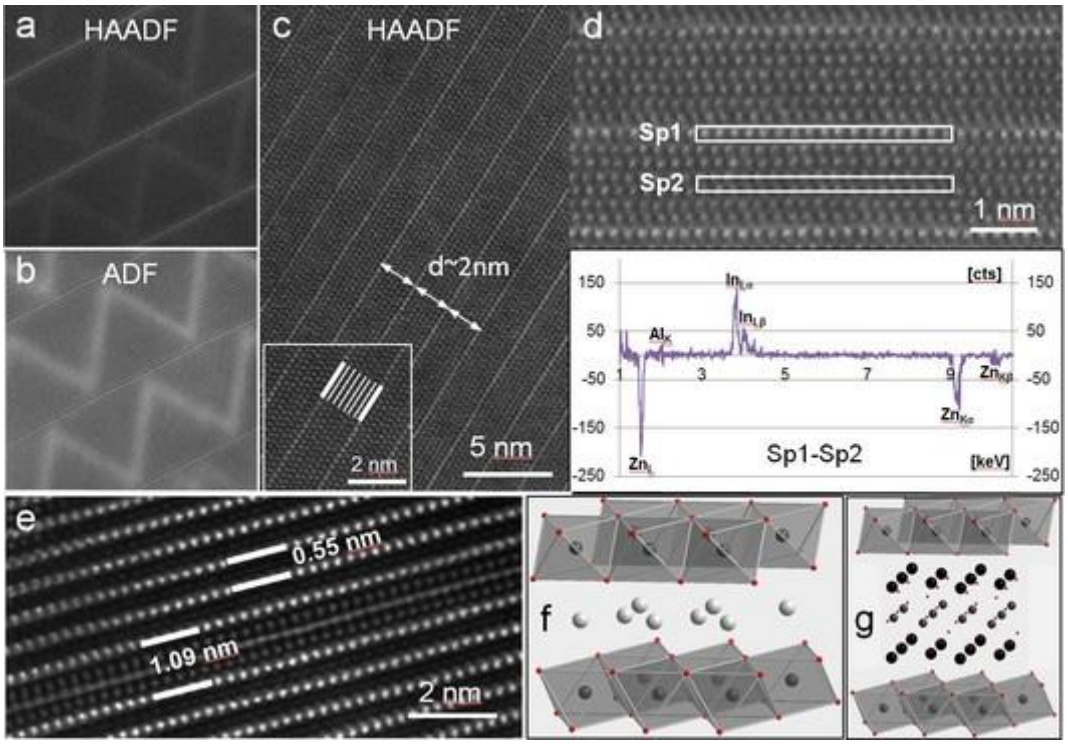

Figure 2. (a) HAADF STEM image of In-rich basal IB's. (b) ADF imaging revealing the pyramidal IB's. (c) Ordered IB's corresponding to $(ZnO)_5.In_2O_3$ phase. (d) Region of EDS analysis and spatial difference spectrum. (e) Intergrowth of $Ca_3Co_4O_9$-Na_xCoO_{2+x} layered cobaltates. (f) $NaxCoO_{2+x}$ structure and (g) $Ca_3Co_4O_9$ structure.

References:

1. S.N. Ruddlesden, P. Popper, Acta Crystallogr. 11 (1958) 54-55.
2. A. Rečnik et al., J. of the European Ceram. Soc. 27(4) (2007) 1999-2008.
3. D. Vengust et al., Chem. Mater. 25 (2013) 4791-4797.